

# Rigorous Analysis of Software Countermeasures against Cache Attacks

Goran Doychev  
*IMDEA Software Institute*  
 goran.doychev@imdea.org

Boris Köpf  
*IMDEA Software Institute*  
 boris.koepf@imdea.org

## Abstract

CPU caches reduce the latency of memory accesses on average, but not in the worst case. Thus, they introduce variations into the execution time that can be exploited by adversaries to recover secrets from programs, such as private information about users or cryptographic keys.

Establishing the security of countermeasures against this threat often requires intricate reasoning about the interactions of the program and the hardware platform and has so far only been done for restricted cases.

In this paper we devise novel techniques that provide support for bit-level and arithmetic reasoning about pointers in the presence of dynamic memory allocation. These techniques enable us to perform the first rigorous analysis of widely deployed software countermeasures against cache attacks on modular exponentiation, based on executable code.

## 1 Introduction

CPU caches reduce the latency of memory accesses on average, but not in the worst case. Thus, they introduce variations into the execution time that can be exploited by adversaries to recover secrets from programs, such as private information about users or cryptographic keys.

A large number of techniques have been proposed to counter this threat. Some proposals work at the level of the operating system [13], others at the level of the hardware architecture [22] or the cryptographic protocol [11]. However, so far only software countermeasures have seen wide-spread adoption in practice.

The most defensive countermeasure is to forbid control flow, memory accesses, and execution time of individual instructions to depend on secret data. While such code is easily seen to prevent leaks through instruction and data caches, it also prevents the performance gains enabled by such accelerators. More permissive countermeasures are to ensure that both branches

of each conditional fit into a single line of the instruction cache, to preload lookup tables, or to permit secret-dependent memory access patterns as long as they are secret-independent at the granularity of cache lines or sets. Such permissive code can benefit from hardware acceleration, however, analyzing its security requires intricate reasoning about the interactions of the program and the hardware platform and has so far only been done for restricted cases.

A major hurdle for reasoning about such interactions is that it requires support for accurate, logical and arithmetic reasoning on pointers (for tracking cache alignment), but it also requires dealing with pointers symbolically (for capturing dynamically allocated memory used by multi-precision integer arithmetic). In this paper we present novel reasoning techniques that support both features. Based on these techniques we devise novel abstractions that capture a range of adversary models, including those that can observe sequences of accessed addresses, or those that can observe sequences of accessed memory blocks. We frame both contributions in terms of novel abstract domains, which we implement on top of the CacheAudit static analyzer [10].

We evaluate the effectiveness of our techniques in a case study where we perform the first formal analysis of commonly used software countermeasures for protecting modular exponentiation algorithms against cache side channels. The paper contains a detailed description of our case study; here we highlight the following results:

- We analyze the security of the scatter/gather countermeasure used in OpenSSL 1.0.2f for protecting window-based modular exponentiation. Scatter/gather ensures that the pattern of data cache accesses is secret-independent at the level of granularity of cache lines and, indeed, our analysis of the binary executables reports security against adversaries that can monitor only cache line accesses.
- Our analysis of the scatter/gather countermeasure

also reports a leak with respect to adversaries that can monitor memory accesses at a more fine-grained resolution. This weakness that has been exploited in the CacheBleed attack [24], where the adversary observes accesses to the individual banks within a cache line. We analyze the variant of scatter/gather published in OpenSSL 1.0.2g as a response to the attack and prove its security with respect to powerful adversaries that can monitor the full address trace.

- Our analysis detects the side channel in the square-and-multiply based algorithm in libgrypt 1.5.2 that has been exploited in [23, 16], but can prove the absence of instruction and data cache leaks in the square-and-*always*-multiply algorithm used in libgrypt 1.5.3, for some compiler optimization levels.

Overall, our results illustrate the dependency of software countermeasures against cache attacks on brittle details of the compilation and the hardware architecture, and they demonstrate how the techniques developed in our paper can effectively support rigorous analysis of software countermeasures.

In summary, our contributions are to devise novel techniques that enable cache-aware reasoning about dynamically allocated memory, and to put these techniques to work in the first rigorous analysis of widely deployed permissive countermeasures against cache side channel attacks.

The remainder of this paper is structured as follows. In Section 2 we illustrate the scope of our techniques by example. In Section 3 we define programs and adversaries that observe them. In Section 4 and 5 we define our novel abstract domains. We present our case studies in Section 6 before we revisit prior art and conclude in Sections 7 and 8, respectively.

## 2 Illustrative Example

We illustrate the scope of the techniques developed in this paper using a problem that arises in implementations of windowed modular exponentiation. There, powers of the base are pre-computed and stored in a table for future lookup. Figure 1 shows an example memory layout of two such pre-computed values  $p_1$  and  $p_2$ , each of 3072 bits. An adversary that observes accesses to the six memory blocks starting at 80eb140 knows that  $p_2$  was requested, which can give rise to effective key-recovery attacks [16].

Defensive approaches for table lookup, as implemented in NaCl or libgrypt 1.6.3, avoid such vulnerabilities by accessing *all* table entries, in a constant order.

80eb140	00 00 00 00 00 00 01 89	66 07 7e bd 53 8d 2f 3e
80eb150	08 e0 7c de 16 09 e0 20	db 1d 94 71 65 ca 35 4b
80eb160	6c 35 61 ac ec 74 80 20	b7 9e e9 76 c0 f1 f9 9a
80eb170	df b3 ac 9d ad fa 98 35 93 c3 5f ef 3c ac f9 df	
80eb180	ec 6c 94 45 60 ad 03 e0 7a 03 66 4e 60 17 5d 8b	
80eb2b0	0e b7 c1 83 76 09 6d 95 62 20 e2 5b 31 1a 00 d8	
80eb2c0	e7 d5 a6 a4 2d 41 2e 55 00 00 00 00 00 01 89	
80eb2d0	1f ca 10 9d 92 26 d0 00 aa ca d9 d0 23 bc 94	
80eb2e0	b2 ba 4c e6 19 d5 d0 44 e6 5b 86 cf c9 3e e8	
80eb2f0	de dc cd 46 6d b1 61 6c 4b 58 df 2f ad a6 99 f7	
80eb300	86 c1 05 f8 83 89 4a 53 a8 c9 d0 da fd 7f 50 7e	
80eb430	7e 61 30 7c c4 10 b3 2a 85 5c fc fb 3c 07 29 86	
80eb440	ac 9a 2a 5f 73 c7 80 75 80 68 be 98 0b e3 49 ba	

Figure 1: Layout of pre-computed values in main memory, for the windowed modular exponentiation implementation from libgrypt 1.6.1. Data highlighted in different colors correspond to the pre-computed values  $p_2$  and  $p_3$ , respectively. Black lines denote the memory block boundaries, for an architecture with blocks of 64 bytes.

OpenSSL 1.0.2f instead uses a more permissive approach that accesses only *one* table entry, however it uses a smart layout of the tables to ensure that the requested memory blocks are loaded into cache in a constant order. An example layout for storing 8 pre-computed values is shown in Figure 2. The code that manages such tables consists

	$p_{2,0}$	$p_{1,0}$	$p_{0,0}$	$p_{7,0}$	$p_{4,0}$	$p_{3,1}$	$p_{0,1}$	$p_{7,1}$	$p_{4,1}$
80eb140	9d bd 4c af e8 3f 74 6e 10 7e d1 76 78 d2 a2 3d								
80eb150	ca 07 96 c8 be 8d 43 7e 1f 66 07 cb 6e 4a 1f 00								
80eb160	cd 3e da 88 1e ff 0d dd ca 2f 8c c7 88 32 91 02								
80eb170	26 8d ab cc e1 06 7f f7 92 53 6f cc 00 fd d5 17								
80eb180	d9 de 4c e9 30 7f d6 8f ca 7c 07 6f f6 62 47 84								
80eb190	aa e0 1b b4 93 7e a6 81 00 08 fa ea 57 6c 8f 86								
80eb1a0	94 b0 4c 93 3f 2a 23 10 bc e0 f0 75 22 85 62 d9								
80eb1b0	23 09 b5 51 32 4f 15 df d0 16 d7 44 d6 01 73 3d								
80eb1c0	5f 5b a7 eb 4c 74 3a ae 2a e2 ff 26 82 15 34 cf								
80eb1d0	9a 20 0b 15 4e 0f e4 7c ac 60 93 6d 16 ea 96 85								
80eb1e0	75 d8 cf 86 7e 3d af 57 82 02 57 d0 7e 67 f0 c1								
80eb1f0	c7 1a ec db ce 7a 67 1e 73 31 93 e1 c9 a3 d4 0a								
80eb200	98 a4 6d 74 b1 24 bb 93 be a6 3f 3f 06 cc b2 28								
80eb210	68 d5 5e 23 ab 7f 7a 4b 80 e7 b9 4a 1d be 26 01								
80eb220	b4 55 65 aa 35 29 22 57 49 2e 67 79 5c 54 f8 dc								
80eb230	e3 41 7f 7a 45 44 f1 a4 0b 2d ac 55 89 f6 a5 80								

Figure 2: Layout of pre-computed values in main memory, achieved with the scatter/gather countermeasure. Data highlighted in different colors correspond to pre-computed values  $p_0, \dots, p_7$ , respectively. Black lines denote the memory block boundaries, for an architecture with blocks of 64 bytes.

of three functions, which are given in Figure 3.

- To create the layout, the function `align` aligns a buffer of memory with the memory block boundary by ensuring the least-significant bits of the buffer address are zeroed, see Figure 3a.
- To write a value into the array the function `scatter` ensures that the bytes of the pre-com-

puted values are stored `spacing` bytes apart, see Figure 3a.

- Finally, to retrieve a pre-computed value from the buffer, the function `gather` assembles the value by accessing its bytes in the same order they were stored, see Figure 3c.

```
(1) align(buf)
(2)   return buf - buf & (block_sz - 1) + block_sz
      (a) Aligning a buffer with block boundary.

(1) scatter(buf, p, k)
(2)   for i := 0 to N - 1 do
(3)     buf[k + i * spacing] := p[k][i]
      (b) Storing a pre-computed value into a buffer.

(1) gather(r, buf, k)
(2)   for i := 0 to N - 1 do
(3)     r[i] := buf[k + i * spacing]
      (c) Retrieving a pre-computed value from a scattered buffer.
```

Figure 3: Scatter/gather method for storing and retrieving pre-computed values.

Reasoning about the effectiveness of such countermeasures is a daunting task, involving reasoning about the interactions of the program and the hardware platform. First, one must ensure that the compiler does not perform unexpected optimizations. Second, one must ensure that the data is aligned correctly, considering the memory and cache geometry, e.g. considering the size of the cache lines. Third, one must ensure that the assertions hold when considering unknown dynamic locations in memory, as practical implementations place the pre-computed values in heap memory.

The techniques we develop in this paper enable, for the first time, the rigorous security analysis of permissive countermeasures against side-channel attacks, such as the one in Figure 3, based on executable code. Specifically, our techniques enable the static analysis of basic logical and arithmetic operations on symbolic values, which is required for reasoning about cache alignment in the presence of dynamically allocated memory in functions such as `align`, `scatter`, and `gather`. We further develop techniques for tracking sets of observations of cache adversaries, and for computing their size, which enables the quantification of leaks. The results we derive are quantitative upper bounds on the information leaked to different kinds of adversaries; they include formal proofs of non-leakage, but go beyond them in that they help shed insights into the severity of leaks, should they exist.

### 3 Security Against Memory Trace Attacks

In this section we define three kinds of adversaries that can monitor a program’s accesses to main memory, ranked by their observational capabilities. We begin by introducing abstract notions of programs and computations.

#### 3.1 Programs and Computations

A program  $P = (\Sigma, I, \mathcal{A}, \mathcal{T})$  consists of the following components:

- $\Sigma$  - a set of *states*
- $I \subseteq \Sigma$  - a set of *initial* states
- $\mathcal{A}$  - a set of *addresses*
- $\mathcal{T} \subseteq \Sigma \times \mathcal{A}^* \times \Sigma$  - a *transition relation*

A *transition*  $(\sigma_i, a, \sigma_j) \in \mathcal{T}$  captures two aspects of a computation step: first it describes how the instruction set semantics operates on data stored in CPU registers and main memory, namely by updating  $\sigma_i$  to  $\sigma_j$ ; second it describes the sequence of memory accesses  $a \in \mathcal{A}^*$  issued during this update, which includes the addresses accessed when fetching instructions from the code segment, as well as the addresses containing accessed data.

A *computation* of  $P$  is an alternating sequence of states and events  $\sigma_0 a_0 \sigma_1 a_1 \dots \sigma_n$  such that  $\sigma_0 \in I$ , and that for all  $i \in \{0, \dots, n-1\}$ ,  $(\sigma_i, a_i, \sigma_{i+1}) \in \mathcal{T}$ . The set of all computations of  $P$  is its *trace collecting semantics*  $Col(P) \subseteq Traces$ . When considering terminating programs, the trace collecting semantics can be formally defined as the least fixpoint of the *next* operator containing  $I$ :

$$Col(P) = I \cup next(I) \cup next^2(I) \cup \dots,$$

where *next* describes the effect of one computation step:

$$next(S) = \{t.\sigma_n a_n \sigma_{n+1} \mid t.\sigma_n \in S \wedge (\sigma_n, a_n, \sigma_{n+1}) \in \mathcal{T}\}$$

In the rest of the paper, we assume that  $P$  is fixed and abbreviate its trace collecting semantics by *Col*. Moreover, we will consider only  $P$  that are deterministic and terminating.

#### 3.2 A Hierarchy of Memory Trace Observers

We define three notions of security against memory trace attacks, corresponding to different observational capabilities of the adversary. We express these capabilities in terms of *views*, which are functions that map traces in *Col* to the set of observations an adversary can make.

The views can be derived by successively applying lossy transformations to the sequence of memory accesses of a program, which leads to a hierarchy of security definitions.

**Address-trace observer** The first adversary we consider is one that can observe the full sequence of memory locations that are accessed. Security against this adversary implies resilience to many kinds of microarchitectural side channels, through cache, TLB, DRAM, and branch prediction buffer.<sup>1</sup> This observer, when restricted to addresses of instructions, is equivalent to the program counter security model [20].

Formally, we define the address-trace observer by the view which takes the initial state and returns the exact sequence of accessed addresses in memory:

$$view^{ato} : \sigma_0 a_0 \sigma_1 a_1 \dots \sigma_n \mapsto a_0 a_1 \dots a_{n-1} .$$

**Block-trace observer** The second adversary is one that can observe the sequence of memory blocks loaded by the user to the cache. Security against this adversary implies resilience against adversaries that can monitor memory accesses at the level of granularity of cache lines.

For the formalization, recall that the cache logic splits the bit-representation of an  $n$ -bit memory address in two parts: the least significant  $\log_2 b$  bits represent the position of the address within a memory block of  $b$  bytes, and the most significant  $n - \log_2 b$  bits represent the set index (identifying the cache set) and the tag (identifying data within a cache set).



The projection of an address  $a$  to the most significant  $n - \log_2 b$  bits, denoted by  $block(a)$ , hence gives a formal account of the observation an adversary makes by observing memory addresses at the granularity of blocks. The block-trace observer is then defined by

$$view^{bto} = (mapblock) \circ view^{ato} ,$$

where  $mapblock$  is the natural lifting of  $block$  to sequences.

Note that security against the block-trace observer does not exclude side-channel attacks by adversaries that can make more precise observations about memory accesses, e.g. by observing DRAM or cache bank accesses. Our analysis is easily adapted to capture such adversaries by including more or less bits into the projection of the address, see the discussion of the CacheBleed attack in Section 6.

<sup>1</sup>We do not model, or make assertions about, the influence of advanced features such as out-of-order-execution.

**B-block trace observer** Finally we consider a class of adversaries that can observe a sequence of memory blocks, but that can only make limited observations about repeated accesses to the same memory block (which we call *stuttering*). This captures that the adversary cannot count the number of executed instructions, as long as they are guaranteed not to access main memory<sup>2</sup>; it is motivated by the fact that the latency of cache misses dwarfs that of cache hits and is hence easier to observe.

We formalize this intuition in terms of a function  $view^{bto}$  that takes as input a sequence  $w$  of blocks and maps maximal subsequences  $b^r$  to the block  $b$ . That is, repetitions of any block are removed.

**Example 1.** The function  $view^{bto}$  maps both  $aabcddc$  and  $abbbccddcc$  to the sequence  $abcdc$ , making them indistinguishable to the adversary.

We also consider a more powerful observer adversary that can distinguish between repetitions of blocks if they exceed a certain number. We omit the technical details for brevity.

### 3.3 Quantifying Leaks

A common approach to quantifying the degree of confidentiality provided by a program is to derive bounds on the number of observations an adversary can make [17, 14]. We follow this approach, and quantify the information leakage (in bits) as

$$\log_2 |view(Col)| . \tag{1}$$

An advantage of this approach is that it can be automated using standard program analysis techniques and that it comes with different interpretations in terms of security: For example, it can be related to a lower bound on the expected number of guesses an adversary has to make for successfully recovering the secret [19], or to an upper bound for the probability of successfully guessing the secret in one shot [21]. A disadvantage of the application of this approach in previous works is that they have not distinguished between variations in adversary observations that are due to secret data and those that are due to public data. Rather, all unknown data has been considered to be secret (see e.g. [10]), which can lead to severe imprecisions of the analysis.

In the language of information flow analysis, secret data is called *high*, and public data is called *low*. In this paper, we propose a novel approach to handle low data by introducing *symbolic values*, which are values that are not known in advance but do not contain secrets. If a

<sup>2</sup>Here we rely on the (weak) assumption that the second  $b$  in any access sequence  $\dots bb \dots$  is guaranteed to hit the cache.

symbolic value is part of the adversary’s view, the adversary will observe the concrete valuation of the value without learning additional information about the secret data. Thus, symbols take the role of low data, and all remaining variations of the output are potentially due to high data. In that sense, our analysis can be seen as the first quantitative information-flow analysis that can deal with low inputs symbolically. In Section 4, we describe our use of symbolic values to capture pointer arithmetic with unknown (but non-secret) memory locations.

### 3.4 Statically Determining Bounds on Leaks

In this paper, we perform static analysis to determine upper bounds on information leakage as defined in equation (1). However, in order to obtain  $Col$ , a fixpoint of the  $next$  operator is needed, which is practically infeasible in most cases. Abstract interpretation [9] overcomes this fundamental problem by computing a fixpoint with respect to an efficiently computable over-approximation of  $next$ . This new fixpoint represents a superset of all computations, which is sufficient for deriving an upper bound on the range of the channel and thus on the leaked information.

Technically, the effects of computation steps are tracked by the abstract  $next^\sharp$ -operator, and its fixpoint results in an abstract collecting semantics  $Col^\sharp \subseteq Traces^\sharp$ . We obtain upper bounds on leaks by computing  $\log_2 |\text{view}(\gamma(Col^\sharp))|$ , where  $\gamma$  is the *concretization function*, delivering the set of concrete elements represented by an abstract element. The correctness of the derived bounds on leaks is established by the *global soundness* of the analysis, which is defined as

$$Col \subseteq \gamma(Col^\sharp). \quad (2)$$

Informally, the global soundness states that the analysis overapproximates the computations of the program. A central result from [9] states that global soundness is fulfilled if the abstract domains satisfy *local soundness*, which is defined as

$$\forall a \in Traces^\sharp : next(\gamma(a)) \subseteq \gamma(next^\sharp(a)). \quad (3)$$

Informally, local soundness states that the effect of each computation step is overapproximated, in the sense that the computations reachable when applying the abstract  $next^\sharp$ -operator are a superset of the computations reachable when applying the concrete  $next$ -operator.

## 4 Abstract Domain for Cache-Aware Pointer Arithmetic

Cache-aware code often uses Boolean and arithmetic operations on pointers in order to achieve favorable memory alignment. In this section we devise the *masked symbol domain*, which is a simple abstract domain that enables the static analysis of such code in the presence of dynamically allocated memory.

### 4.1 Representation

The masked symbol domain is based on finite sets of what we call *masked symbols*, namely pairs  $(s, m)$  consisting of a *symbol*  $s \in Syms$  and a *mask*  $m \in \{0, 1, \top\}^n$ . The idea is that the symbol  $s$  represents an unknown base address and  $m$  represents the pattern of known and unknown bits. Here,  $\{0, 1\}$  stand for known bits and  $\top$  stands for unknown bits. The  $i$ -th bit of a masked symbol  $(s, m)$  is hence equal to  $m_i$ , unless  $m_i = \top$ , in which case it is unknown. In the first case we call the bit *masked*, in the second *symbolic*. We abbreviate the mask  $(\top, \dots, \top)$  by  $\top$ .

Two special cases of masked symbols are worth pointing out:

1.  $(s, \top)$  represents an unknown constant, and
2.  $(s, m)$  with  $m \in \{0, 1\}^n$  represents the bit-vector  $m$ .

That is, pairs of the form  $(s, m)$  generalize both bitvectors and unknown constants.

### 4.2 Concretization and Counting

We now give a semantics to elements of the masked symbol domain. This semantics is parametrized w.r.t. instantiations of the symbols. For the case where masked symbols represent partially known heap addresses, a valuation corresponds to one specific layout.

Technically, we define the concretization of finite sets  $F \subseteq Syms \times \{0, 1, \top\}^n$  w.r.t. a mapping  $\sigma : Syms \rightarrow \{0, 1\}^n$  taking symbols to bit-vectors:

$$\gamma_\sigma(F) = \{\sigma(s) \oplus m \mid (s, m) \in F\}$$

Here  $\oplus$  is defined bitwise by  $c_i \oplus m_i = m_i$  whenever  $m_i \in \{0, 1\}$ , and  $c_i$  otherwise.

The following proposition shows that precise valuation of the constant symbols can be ignored for deriving upper bounds on the numbers of values that the novel domain represents. It enables the quantification of information leaks in the absence of exact information about locations on the heap.

**Proposition 1.** *For every valuation  $\sigma : Syms \rightarrow B$  we have  $|\gamma_\sigma(F)| \leq |F|$*

Note that, with this definition we do not assume any relationship between symbols. Below we will increase its precision by tracking basic arithmetic relations between symbols.

### 4.3 Update

We support two kinds of operations on elements of the masked symbol domain. The first tracks patterns on bit-vectors and is needed for reasoning about memory alignment. The second tracks the arithmetic relationship between masked symbols and is needed for basic pointer arithmetic and equality checks. Here we describe only operations between individual masked symbols, the lifting to sets is obtained by performing the operations on all pairs of elements.

**Tracking Bits** An important class of operations for cache-aware coding are those that allow the alignment of data to memory blocks without knowing the precise pointer value.

**Example 2.** *The following code snippet allocates 1000 bytes of heap memory and stores a pointer to this chunk in  $x$ .*

```
x = malloc(1000);
y = (x & 0xFFFFF0) + 0x40;
```

*The second line ensures that the 6 least significant bits of that pointer are set to 0, thereby aligning it with cache lines of 64 bytes. Finally, adding 0x40 ensures that the resulting pointer points into the allocated region while keeping the alignment.*

To reason about this kind of code, we distinguish between operations that allow the introduction of a mask and those that maintain a symbol: The left column of Table 1 lists logical bit operations that translate symbolic bits into masked bits, i.e. creating a mask. For example, the operation  $x \ \& \ 0xFFFFF0$  in Example 2 results in a masked symbol

$$(s_x, (\top \cdots \top 000000)). \quad (4)$$

The right column in Table 1 lists logical bit operations that leave symbolic bits unmodified, thus maintaining the symbol. Information about the mask can also be maintained throughout arithmetic operations such as additions, as long as all carry bits can be absorbed within the mask. For example, the addition of 0x3F to (4) results in a masked symbol

$$(s_x, (\top \cdots \top 111111)),$$

for which we can statically determine containment in the same cache line as  $(s_x, (\top \cdots \top 000000))$ .

$s \ \& \ 0 = 0$	$s \ \& \ 1 = \top$
$s \   \ 1 = 1$	$s \   \ 0 = \top$
$s \ \wedge \ s = 0$	$s \ \wedge \ 0 = \top$
$s \ - \ s = 0$	

Table 1: Bit operations and their effect on masked symbols. The left column shows operations that recover mask bits from symbols. The right column contains operations that leave symbolic bits unmodified.

In cases when an operation does affect the symbolic bits, we take a conservative approach and drop information about the symbols. Formally,

$$(s_1, m_1) \circ (s_2, m_2) = ((s_3), \top),$$

where  $s_3$  is a fresh symbol. For example, the addition of 0x40 to (4) in Example 2 results in the masked symbol

$$(s_y, (\top \cdots \top 000000)),$$

which points to the beginning of some (unknown) cache line.

**Tracking Arithmetic Relationships** Besides providing support for bit-operations on symbolic addresses we also require support for basic pointer arithmetic.

**Example 3.** *The following code snippet sets the values of array  $A$  for indices  $i = 0, \dots, 9$ .*

```
int *x = A + 10;
int *y;
for (y = A; y <= x; y++)
    *y = get_value (...);
```

*The loop terminates whenever pointer  $y$  points at or beyond  $x$ . While pointer arithmetic here can be avoided by an implementation using an integer counter in the for-condition, modern compilers often optimize such implementations to a form using pointer arithmetic.*

The operations on symbols defined so far are not sufficient for analyzing the code in example 3 in case that  $A$  has a symbolic value. The reason for this is that a fresh symbol is generated at each iteration, and we will not be able to establish that  $*y$  has reached  $A + 10$ . To address this shortcoming, we add support for tracking simple arithmetic congruences between masked symbols. For masked symbols  $x, y$ , those congruences are terms of the form  $x = y + o$ , where  $o$  is an integer constant.

Building up a set of constraints  $C$  between masked symbols means to gather further information about the memory layout. Technically, we model this by defining

the semantics  $\gamma_\sigma(F)$  of a set of masked symbols only w.r.t. symbol valuations  $\sigma: \text{Syms} \rightarrow \{0, 1\}^n$  that satisfy

$$\sigma(s_1) \oplus m_1 = \sigma(s_2) \oplus m_2 + o,$$

for all  $(s_1, m_1) = (s_2, m_2) + o \in S$ . As in Proposition 1, adding constraints improves the precision of counting.

**CPU Flag Values** When performing an update involving masked symbols, CPU flag values may be affected. By default we safely assume that all flag combinations are possible. To improve precision of the analysis, we identify several cases where flags are determined even though values are symbolic. Among those cases, we identify the following:

1. If at least one masked bit of the result is non-zero, then  $ZF = 1$ .
2. If the operation does not affect the (possibly symbolic) most-significant bits of the operands, then  $CF = 0$ .
3. For operations `sub src, dst` (or equivalently, `cmp src, dst`), if we can deduce that `src = dst + c` with  $c \neq 0$ , then  $ZF = 1$ .

A combination of information about the values of flags and arithmetic congruences between pointers enables the analysis to determine when to exit the loop in Example 3.

**Local Soundness** To establish the local soundness (see (3) in Section 3.4) of the masked symbol domain, we consider the abstract  $next^\sharp$ -operator for the domain, which is implemented by the update-function described in this section.

**Lemma 1.** *The masked symbol domain is locally sound.*

Informally, the soundness follows from the soundness of the ingredients of its update: (a) fresh symbols are used whenever exact values are not known; (b) the trivial congruence  $x = x + 0$  is used whenever no congruence between  $x$  and another masked symbol is known; (c) all flag combinations are considered whenever the operation does not determine the exact flags.

## 5 Abstract Domains for Memory Access Traces

In this section, we present data structures for representing the set of possible memory accesses a program can make, and for computing the number of observations that

different side channel attackers can make. For this we devise the *access-trace domains*, which capture the adversary models introduced in Section 3.2: address-trace (adversary who can observe addresses), block-trace (adversary who can observe memory blocks), and b-block-trace (adversary who can observe memory blocks modulo repetitions). We describe those domains, and elaborate on developments which allow us to precisely capture cases where a b-block-trace adversary learns less information than an address- and block-trace adversary, as is the case in the following example.

**Example 4.** *The following code snippet presents implicit information flow from the secret value  $s$  to the public output  $x$ .*

```
if ( s == 1 ) x = 1; else x = 0;
```

Figure 4 shows layout of the code snippet in the binary. Regardless whether the layout of the executable causes the code to fit into one memory block or two, the same sequence of blocks will be loaded into cache.

00580	E8 BB FD	<code>x := 1</code>	24 24 24 24 24 24	01 75 0A	
00590	C7 44 24		14 01 00 00 00 EB 08	C7 44 24 14 00 00	
005a0	00 00 83 7C		24 14 00 75 07 38	D1 86	<code>x := 0</code>
005b0	B8 D3 86 04		08 8B 54 24 14 89 54 24	00 00 00 00 00 00	

(a) The if-branch causes two I-cache accesses to addresses within block 580; The else-branch causes one I-cache access to an address within block 580.

00580	04 24 E8 B9	FD FF FF 89 44	24 18 8B 45 0C 83 C0		
00590	00 00 00 C7	44 24 08 10 00 00 00	00 C7 44 24 14 00 00		
005a0	00	<code>if s == 1</code>	E8 95 FD FF F	<code>x := 1</code>	1C 83
005b0	7C 24 18 01	75 0A	C7 44 24 14 01 00 00 00	EB 08	
005c0	C7 44 24 14	00 00 00 00	83 7C 24 14 00 75 07 58		
005d0	F1 86	<code>x := 0</code>	B8 F3 86 04 08 8B 54 24 14 89		
005e0	54 24		00 00 00 00 04 C7 04 24 F5 86 04 08 E8 1D		
005f0	FD FF FF B8	00 00 00 00	C9 C3 66 90 66 90 66 90		

(b) The if-branch causes two I-cache accesses to addresses within block 580; The else-branch causes one I-cache access to an address within block 5c0. Afterwards, in both cases instructions within block 5c0 will be executed.

Figure 4: Two possible layouts of if-then-else code, compiled with gcc. The highlighted code corresponds to the if-check and jump, the if-branch and the else-branch, respectively. The red curve represents the jump target in the end of the if-branch. Black lines denote block boundaries, for an architecture with 64-byte memory blocks.

### 5.1 Representation

We use a directed acyclic graph (DAG) to compactly represent traces of memory accesses. While a DAG representation can precisely represent a set of traces [10], a counting procedure which does not require enumerating

all traces may lose precision. The representation we devise is precise for the b-block observer, and provides an easy counting procedure.

The DAG has a set of nodes  $N$  representing memory accesses, with a unique root  $r$  and a set of edges  $E \subseteq N \times N$ . We equip each node  $n \in N$  with a label  $L(n)$  that represents the adversary’s view of the node (i.e. addresses or blocks), and a repetition count  $R(n)$  that represents the number of times each address may be repeatedly accessed. We represent labels  $L(n)$  using the masked symbols abstract domain (see Section 4), and use a finite set abstraction to represent  $R(n)$ .

## 5.2 Concretization and Counting

In an access-trace domain, each node  $n$  represents the set of traces of the program up to this point of the analysis. Its concretization function is defined as

$$\gamma(n) = \bigcup_{\substack{r=n_0 \dots n_k=n \\ \text{path from } r \text{ to } n}} \{\ell_0^{t_0} \dots \ell_k^{t_k} \mid \ell_i \in L(n_i), t_i \in R(n_i)\} \quad (5)$$

For quantitatively assessing leaks we are interested in the number of observations  $|\gamma(n)|$  an adversary can make. An upper bound on this number is easily computed from the access-trace domains using the following recursive equation:

$$\text{count}(n) = |R(n)| \cdot |L(n)| \cdot \sum_{(s,n) \in E} \text{count}(s) \quad (6)$$

For the b-block trace observer, we replace the factor  $|R(n)|$  from the expression in (6) by 1, which captures that this observer cannot distinguish between repetitions of accesses to the same memory block.

## 5.3 Update and Join

The access-trace domains are equipped with functions for update and join, which govern how sets of traces are extended and merged, respectively. The domains are defined with respect to an observer modelled by the  $\text{view} \in \{\text{view}^{\text{ato}}, \text{view}^{\text{bto}}, \text{view}^{\text{bbto}}\}$ , for the different views introduced in Section 3.3. Below we overload the notation of  $\text{view}$  to take as input sets of addresses, and return the respective set of observations (i.e. addresses or blocks).

The *update* receives a node  $n$  representing a set of traces of memory accesses, and it extends  $n$  by a new access to a potentially unknown address that represented a finite set of masked symbols  $F$ . Technically:

1. If the set of masked symbols is not a repetition (i.e. if  $L(n) \neq \text{view}(F)$ ) the update function appends a new node  $n'$  to  $n$  (adding  $(n, n')$  to  $E$ ) and it sets  $L(n') = \text{view}(F)$  and  $R(n') = \{1\}$ .

2. Otherwise (i.e. if  $L(n) = \text{view}(F)$ ) it increments the possible repetitions in  $R(n)$  by one.

The local soundness (see (3) in Section 3.4) of the access-trace domains follows directly because the abstract and the concrete updates are the same, with the difference that the abstract update results in a more compact representation in case of repetitions.

**Lemma 2.** *The access-trace domains are locally sound.*

The *join* for two nodes  $n_1, n_2$  first checks whether those nodes have the same parents and the same label, in which case  $n_1$  is returned, and their repetitions are joined. Otherwise a new node  $n'$  with  $L(n') = \{\varepsilon\}$  is generated and edges  $(n_1, n')$  and  $(n_2, n')$  are added to  $E$ .

To increase precision in counting for the b-block adversary, joins are delayed until the next update is performed. This captures cases where an if-then-else statement spans two memory blocks, both of which are accessed regardless whether if-condition is taken or not, as demonstrated in Figure 4b.

## 6 Case Study

In this section we present a case study in which we leverage the techniques developed in this paper for the first rigorous analysis of several countermeasures against cache side channel attacks against modular exponentiation algorithms from versions of libcrypto and OpenSSL from April 2013 to March 2016. We report on results for leakage to the adversary models presented in Section 3.2 due to instruction-cache (I-cache) accesses and data-cache (D-cache) accesses.<sup>3</sup> As the adversary models are ordered according to their observational capabilities, this sheds light into the level of provable security that different protections offer.

### 6.1 Tool building

We implement the novel abstract domains described in Sections 4 and 5 on top of the CacheAudit open source static analyzer [10]. CacheAudit provides infrastructure for parsing, control-flow reconstruction, and fixed point computation. Our novel domains extend the scope of CacheAudit by providing support for (1) the analysis of dynamically allocated memory, and for (2) adversaries who can make fine-grained observations about memory accesses. The resulting extensions to CacheAudit will be made publicly available.

<sup>3</sup>We also analyzed the leakage from accesses to shared instruction- and data-caches; for the analyzed instances, the leakage results were consistently the maximum of the I-cache and D-cache leakage results.



## 6.2 Target Implementations

For libcrypto we consider versions 1.5.2 to 1.6.3. In those versions of libcrypto, four variants of modular exponentiation are implemented, with different protections against side-channel attacks. In addition to those implementations, we analyze two side-channel protections introduced in OpenSSL versions 1.0.2f and 1.0.2g, respectively. For fairness of comparison of security and performance we implement all protections on top of libcrypto 1.6.3 and analyze this code instead of OpenSSL.

To generate the target executables of our experiments, we use ElGamal decryption routines based on each of the above-described implementations of modular exponentiation and the respective countermeasures, resulting in 5 implementations. We compile them using GCC 4.8.4, on a 32-bit Linux machine running kernel 3.13. For ElGamal decryption, we use a key size of 3072 bits.

The current version of CacheAudit supports only a subset of the x86 instruction set and CPU flags, which we extend on demand. To bound the required extensions we focus our analysis on the regions of the executables that were targeted by exploits and to which the corresponding countermeasures were applied, rather than the whole executables. As a consequence, the formal statements we derive only hold for those regions. In particular, we do not analyze the code of the libcrypto’s multi-precision integer multiplication and modulo routines, and we specify that the output of the memory allocation functions (e.g. `malloc()`) is symbolic (see Section 4).

## 6.3 Square-and-Multiply Modular Exponentiation

The first target of our analysis is modular exponentiation by square-and-multiply. The algorithm is depicted in Figure 5 and is implemented, e.g., in libcrypto version 1.5.2. Line 5 of the algorithm contains a conditional branch whose condition depends on a bit of the secret exponent. An attacker who can observe the victim’s accesses to instruction or data caches may learn which branch was taken and identify the value of the exponent bit. This weakness has been shown to be vulnerable to key-recovery attacks based on prime+probe [16, 25] and flush+reload [23].

In response to these attacks, libcrypto 1.5.3 implements a countermeasure that makes sure that the squaring operation is always performed, see Figure 6 for the pseudocode. It is noticeable that this implementation still contains a conditional branch that depends on the bits of the exponent in Line 7, namely the copy operation that selects the outcome of both multiplication operations. However, this has been considered a minor problem because the branch is small and is expected to fit into the

same cache line as preceding and following code, or to be always loaded in cache due to speculative execution [23]. In the following we apply the techniques developed in this paper to analyze whether the expectations on memory layout are met.

```
(1) r := 1
(2) for i := |e| - 1 downto 0 do
(3)   r := mpi_sqr(r)
(4)   r := mpi_mod(r, m)
(5)   if e_i = 1 then ← vulnerable conditional jump
(6)     r := mpi_mul(b, r)
(7)     r := mpi_mod(r, m)
(8) return r
```

Figure 5: Pseudocode for square-and-multiply modular exponentiation

```
(1) r := 1
(2) for i := |e| - 1 downto 0 do
(3)   r := mpi_sqr(r)
(4)   r := mpi_mod(r, m)
(5)   tmp := mpi_mul(b, r)
(6)   tmp := mpi_mod(tmp, m)
(7)   if e_i = 1 then
(8)     r := tmp
(9) return r
```

Figure 6: Pseudocode for square-and-always-multiply modular exponentiation

Observer	address	block	b-block
I-Cache	1 bit	1 bit	1 bit
D-Cache	1 bit	1 bit	1 bit

(a) Square-and-multiply from libcrypto 1.5.2

Observer	address	block	b-block
I-Cache	1 bit	1 bit	0 bit
D-Cache	0 bit	0 bit	0 bit

(b) Square-and-always-multiply from libcrypto 1.5.3

Figure 7: Leakage of modular exponentiation algorithms to observers of instruction and data caches, with cache line size of 64 bytes and compiler optimization level `-O2`.

**Results** The results of our analysis are given in Figure 7 and Figure 9

- Our analysis identifies a 1-bit data cache leak in square-and-multiply exponentiation, see line 2 in

Observer	address	block	b-block
I-Cache	1 bit	1 bit	1 bit
D-Cache	1 bit	1 bit	1 bit

Figure 8: Leakage of square-and-always-multiply from libgcrypt 1.5.3, with cache line size of 32 bytes and compiler optimization level  $-O0$ .

Figure 7a, which is due to memory accesses in the conditional branch in that implementation. Our analysis confirms that this data cache leak is closed by square-and-always-multiply, see line 2 in Figure 7b

- Line 1 of Figures 7a and Figure 7b show that both implementations leak through instruction cache to powerful adversaries who can see each access to the instruction cache. However, for weaker, b-block observers that cannot distinguish between repeated accesses to a block, square-and-always-multiply does *not* leak, confirming the intuition that the conditional copy operation is indeed less problematic than the conditional multiplication.
- The data in Figure 8 demonstrates that the advantages of conditional copy over conditional multiplication depend on details such as cache line size and compilation strategy. Figure 9 illustrates this effect for the conditional copy operation, where more aggressive compilation leads to more compact code that fits into single cache lines. The same effect is observable for data caches, where more aggressive compilation avoids data cache accesses altogether.

## 6.4 Windowed Modular Exponentiation

In this section we analyze windowed algorithms for modular exponentiation. These algorithms differ from algorithms based on square-and-multiply in that they process multiple exponent bits in one shot. For this they commonly rely on tables filled with precomputed powers of the base. For example, libgcrypt 1.6.1 precomputes 7 multi-precision integers and handles the power 1 in a branch, see Figure 10. For moduli of 3072 bits, each precomputed value requires 384 bytes of storage which amounts to 6-7 memory blocks in architectures with cache lines of 64 bytes. Key-dependent accesses to those tables can be exploited for mounting cache side channel attacks [16].

41a80	8b 54 24 30 c1 e	jne 41AA1	84 24 80 00 00 00
41a90	8b 84 24 80 00 00		00 00 85 c0 75 c6 89 e8 89 fd 89
41aa0	c7 83 ea 01 89 f0		d1 64 24 18 85 d2 0f 85 ef fe
41ab0	ff ff 83 6c 24 28		01 0f 89 d0 fe ff ff 89 c6 8b

(a) Compiled with the default gcc optimization level  $-O2$ . Regardless whether the jump is taken or not, first block 41a80 is accessed, followed by block 41aa0. This results in a 0-bit b-block leak.

5d040	8b 45 9c c1 e8 1f	je 5D081	84 24 80 00 00 00
5d050	89 05 2c ff ff ff		8b 05 2c ff ff ff 05 c0 74 21
5d060	8b 85 30 ff ff ff		89 45 d4 8b 45 94 89 85 50 ff
5d070	ff ff 8b 45 d4 00		45 94 8b 45 a0 89 85 48 ff ff
5d080	ff d1 65 9c 83 6d		98 01 83 7d 98 00 0f 85 7e ff
5d090	ff ff 83 6d 90 01		83 7d 90 00 79 0d 90 83 7d c4

(b) Compiled with gcc optimization level  $-O0$ . The memory block 5d060 is only accessed when the jump is taken. This results in a 1-bit b-block leak.

Figure 9: Layout of libgcrypt 1.5.3 executables with 32-byte memory blocks (black lines denote block boundaries). The highlighted code corresponds to the conditional branching in lines 7–8 in Figure 6. The red region corresponds to the executed instructions in the if-branch. The blue curve points to the jump target, where the jump is taken if the if-condition does not hold.

```

if (e0 == 0) {
    base_u = bp;
    base_u_size = bsize;
} else {
    base_u = b_2i3[e0 - 1];
    base_u_size = b_2i3size[e0 - 1];
}

```

Figure 10: Sliding window table lookup from libgcrypt 1.6.1. Variable  $e0$  represents the window, right-shifted by 1. The lookup returns a pointer to the first limb of the multi-precision integer in  $base\_u$ , and the number of limbs in  $base\_u\_size$ . The first branch deals with powers of 1 by returning pointers to the base.

We consider three countermeasures, which are commonly deployed to defend against this vulnerability. They have in common that they all *copy* the table entries instead of returning a pointer to the entry.

- The first countermeasure ensures that in the copy process, a constant sequence of memory locations is accessed, see Figure 11 for pseudocode. The expression on line 7 ensures that only the  $k$ -th pre-computed value is actually copied to  $r$ . This countermeasure is implemented, e.g. in NaCl and libgcrypt 1.6.3.
- The second countermeasure stores precomputed

```

(1) // Retrieves r from p[k]
(2) defensive_retrieve(r, p, k)
(3)   for i := 0 to n - 1 do
(4)     for j := 0 to N - 1 do
(5)       v := p[i][j]
(6)       s := (i == k)
(7)       r[j] := r[j] ^ ((0 - s) & (r[j] ^ v))

```

Figure 11: A defensive routine for array lookup with a constant sequence of memory accesses, as implemented in libgcrypt 1.6.3.

values in such a way that the  $i$ -th byte of all pre-computed values reside in the same memory block. This ensures that when the precomputed values are retrieved, a constant sequence of memory blocks will be accessed. This so-called scatter/gather technique is described in detail in Section 2, with code in Fig 3, and is deployed, e.g. in OpenSSL 1.0.2f.

- The third countermeasure is a variation of scatter/gather, and ensures that the gather-procedure performs a constant sequence of memory accesses (see Figure 12). This countermeasure was recently introduced in OpenSSL 1.0.2g, as a response to the CacheBleed attack [24].

```

(1) defensive_gather(r, buf, k)
(2)   for i := 0 to N - 1 do
(3)     r[i] := 0
(4)     for j := 0 to spacing - 1 do
(5)       v := buf[j + i * spacing]
(6)       s := (k == j)
(7)       r[i] := r[i] | (v & (0 - s))

```

Figure 12: A defensive implementation of gather (compare to Figure 3c) from OpenSSL 1.0.2g.

**Results** Our analysis of the different versions of the table lookup yields the following results:<sup>4</sup>

- Figure 13a shows the results of the analysis of the unprotected table lookup of Figure 10. The leakage of one bit for most adversaries is explained by the fact that they can observe which branch is taken. The layout of the conditional branch is demonstrated in Figure 14a; lowering the optimization level results in a different layout (see Figure 14b), and in this case our analysis shows that the I-Cache b-block leak is eliminated.

<sup>4</sup>We note sliding window exponentiation exhibits further control-flow vulnerabilities, some of which we also analyze. To avoid redundancy with Section 6.3, we focus the presentation of our results on the lookup-table management.

- More powerful adversaries that can see the exact address can learn  $\log_2 7 = 2.8$  bits per access. The static analysis is not precise enough to determine that the lookups are correlated, hence it reports that at most 5.6 bits are leaked.
- Figure 13b shows that the defensive copying strategy from libgcrypt 1.6.3 (see Figure 11) eliminates all leakage to the cache.
- Figure 13c shows that the scatter/gather copying-strategy eliminates leakage for any adversary that can observe memory accesses at the granularity of memory blocks, and this constitutes the first proof of security of this countermeasure. For adversaries that can see the full address-trace, our analysis reports a 3 bit leakage for each memory access, which is again accumulated over correlated lookups because of imprecisions in the static analysis. Below we comment on these results in the context of the recent CacheBleed attack.
- Figure 13d shows that defensive gather introduced OpenSSL 1.0.2g (see Figure 12) eliminates all leakage to cache.

Observer	address	block	b-block
I-Cache	1 bit	1 bit	1 bit
D-Cache	5.6 bit	1 bit	1 bit

(a) Instruction- and Data-Cache leakage of secret-dependent table lookup in the modular exponentiation implementation from libgcrypt 1.6.1.

Observer	address	block	b-block
I-Cache	0 bit	0 bit	0 bit
D-Cache	0 bit	0 bit	0 bit

(b) Instruction- and Data-Cache leakage in the patch from libgcrypt 1.6.3.

Observer	address	block	b-block
I-Cache	0 bit	0 bit	0 bit
D-Cache	1152 bit	0 bit	0 bit

(c) Instruction- and Data-Cache leakage in the scatter/gather technique, applied to libgcrypt 1.6.1.

Observer	address	block	b-block
I-Cache	0 bit	0 bit	0 bit
D-Cache	0 bit	0 bit	0 bit

(d) Instruction- and Data-Cache leakage in the defensive gather technique from OpenSSL 1.0.2g, applied to libgcrypt 1.6.1.

Figure 13: Instruction and data cache leaks of different table lookup implementations. Note that the leakage in Fig 13a accounts for copying a pointer, whereas the leakage in Fig 13b and 13c refers to copying multi-precision integers.

```

4b980  8B 84 24 00 00 00 00 83 EE 01 89 84 24 94 00 00
4b990  00 75 je 4BA58 80 89 6C 24 44 8B 54 24 48 83
4b9a0  E2 0F 0F 84 B0 00 06 06 8D 4A FF 8B 94 8C B8 00
4b9b0  00 00 8B 8C 8C F4 00 00 00 8B 74 24 24 89 44 24
4b9c0  04 8B 44 24 40 89 54 24 03 8B 54 24 28 89 4C 24
4b9d0  0C 89 74 24 18 8B 74 24 1C 89 04 24 8B 44 24 44
4b9e0  89 74 24 14 8B 74 24 20 89 74 24 10 E8 CF F6 FF
4b9f0  FF 8B 84 24 98 00 06 06 89 84 24 94 00 00 00 E9
4ba00  84 FE FF FF 8D 74 26 03 83 6C 24 3C 01 0F 88 7B
4ba10  03 00 00 BF 20 00 00 00 8B 6C 24 3C 2B 7C 24 34
4ba20  89 FA 8B 7C 24 58 8C 0C 16 89 54 24 38 89 4C 24
4ba30  30 8B 3C AF 8B 6C 24 2C 89 FA D3 EA 0F B6 4C 24
4ba40  38 D3 ED 8B 4C 24 34 09 EA 29 F1 D3 E7 89 7C 24
4ba50  2C E9 B5 FE FF FF 66 90 8B 4C 24 4C 8B 54 24 54
4ba60  E9 54 FF FF FF 8B 74 24 44 8B 54 24 40 89 74 24
4ba70  40 8D B4 24 98 00 00 00 89 54 24 44 89 74 24 28

```

(a) Compiled with the default gcc optimization level `-O2`. If the jump is taken, first block `4b980`, followed by block `4ba40`, followed by `4b980` again. If the branch is not taken, only block `4b980` is accessed.

```

47dc0  6C F6 FF FF 8B 84 24 98 00 00 00 89 84 24 94 00
47dd0  00 00 83 FF 01 74 14 09 F0 89 EE 89 C5 EB A9 89
47de0  E8 8B 6C je 47E0B 4 3C EB 04 89 74 24 3C 8B
47df0  54 24 44 83 E2 0F 74 13 83 EA 01 8B 84 94 B8 00
47e00  00 00 8B 94 94 F4 00 00 00 8B 54 24 50 8B
47e10  44 24 58 8D 8C 24 3C 00 00 00 89 4C 24 18 8B 7C
47e20  24 1C 89 7C 24 14 8B 7C 24 20 89 7C 24 10 89 54
47e30  24 0C 89 44 24 08 8B 84 24 94 00 00 00 89 44 24

```

(b) Compiled with gcc optimization level `-O1`. Regardless whether the jump is taken or not, first block `47dc0` is accessed, followed by block `47e00`.

Figure 14: Layout of executables using libgcrypt 1.6.1. The highlighted code corresponds to a conditional branch. The blue region corresponds to the executed instructions in case the if-branch, and the red region corresponds to the executed instructions in the else-branch. Curves represent jump targets.

**The CacheBleed Attack** The recently disclosed CacheBleed attack [24] against the scatter/gather implementation from OpenSSL 1.0.2g exploits timing differences due to *cache-bank conflicts*. Those are possible in CPUs where cache blocks are divided into banks (e.g. Intel Sandy Bridge), to facilitate concurrent accesses to the data cache. For example, the platform targeted in [24] has 16 banks of 4 bytes; there, bits 2–5 of an address are used to determine the bank, and bits 0–1 are used to determine the offset within the bank. The distribution of the pre-computed values in scatter/gather (see Section 2) to different banks will be as shown in Figure 15.

The leak leading to CacheBleed is visible in our data when comparing the results of the analysis with respect to address-trace and block-trace adversaries, however, its severity may be over-estimated due to the powerful address-trace observer. For a more accurate analysis of the effect of cache-bank conflicts, we define the *bank-trace* observer, who cannot distinguish between the elements within a single bank. This observer is weaker than

the address-trace observer, but stronger than the block-trace observer.

We perform the analysis of the scatter/gather implementation (see Figure 13c) for the bank-trace D-cache observer. The analysis results in 384-bit leak, which corresponds to one bit leak per memory access, accumulated for each accessed byte due to analysis imprecision (see above). The one bit leak in the  $i$ -th memory access is explained by the ability of this observer to distinguish between the two banks within which the  $i$ -th byte of all pre-computed values fall.

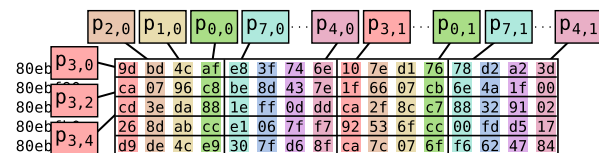


Figure 15: Layout of pre-computed values in cache banks, for a platform with 16 banks of 4-bytes. The cells of the grid represent the cache banks.

## 6.5 Discussion

A number of comments are in order when interpreting the bounds delivered by our analysis.

**Use of Upper Bounds** The results we obtain are upper bounds on the leaked information that are not necessarily tight, that is, they may be pessimistic. This means that while results of zero leakage corresponds to a proof of absence of leaks, positive leakage bounds do not correspond to proofs of the presence of leaks, that is, leaks may be smaller than what is reported by the analysis. The reason for this is that the amount of leaked information may be over-estimated due to imprecisions of the static analysis, as is the case with the D-Cache leak shown on Figure 13c.

**Practical Detectability of Leaks** A reported leak may be practically easier to detect by an adversary in cases where the vulnerable code region produces more cache accesses. This is the case for the control-flow leaks in square-and-multiply, where the vulnerable if-branch includes multiplication and modulo-functions, practically resulting in  $\approx 2 \cdot 10^5$  cache accesses. In contrast, the vulnerable if-branch in square-and-always-multiply does not include function calls, practically resulting in a small number of cache accesses, which may be more difficult to detect from noisy observations.

**Use of Imperfect Models** The guarantees we deliver are only valid to the extent to which the models used

algorithm	square and multiply		sliding window			
	no CM	always multiply	no CM	scatter/gather	access all bytes	defensive gather
original implementation	libgcrypt 1.5.2	libgcrypt 1.5.3	libgcrypt 1.6.1	openssl 1.0.2f	libgcrypt 1.6.3	openssl 1.0.2g
instructions ( $\times 10^6$ )	90.32	120.62	73.99	74.21	74.61	75.29
cycles ( $\times 10^6$ )	75.58	100.73	61.58	61.65	62.20	62.28

Figure 16: Performance of the different versions of modular exponentiation, implemented on top of libgcrypt 1.6.3.

accurately capture the aspects of the execution platform relevant to known attacks. A recent empirical study of OS-level side channels on different platforms [7] shows that advanced microarchitectural features may interfere with the cache, which may render countermeasures ineffective — and formal guarantees invalid.

## 6.6 Performance

We conclude the case study by considering the effect of the different countermeasures on the performance of modular exponentiation. For this, we use libgcrypt 1.6.3 as a base, and we compile it with the respective `mod_exp.c`, corresponding to each of the considered variants. For performance measurement, we use the time for performing exponentiations on a sample of random bases and exponents, and measure the clock count (through the `rdtsc` instruction), as well as the number of performed instructions (through the `PAPI` library). We follow the approach for performance measurement from [12], performing 100,000 exponentiations with exponents, after a warm-up period of 25,000 exponentiations, and take the minimum over 5 repeated experiments to minimize the noise of background processes. The measurements are performed on a machine with an Intel Q9550 CPU. This architecture does not feature more recent performance-enhancing technologies such as Turbo-Boost Technology and Hyper-Threading Technology.

Figure 16 summarizes our measurements. The results show that the applied countermeasure for square and multiply causes a significant slow-down of the exponentiation. A slow-down is observed with sliding-window countermeasures as well, however at a much lower scale.<sup>5</sup> Notable is also the performance gain from using the sliding-window algorithm compared to square-and-multiply.

<sup>5</sup>We note that performance penalties of countermeasures can be higher when considering a whole cryptographic operation, different platforms, implementations within other crypto libraries, different key sizes. For example, in commit messages prior to OpenSSL 1.0.2g’s release, developers report performance penalties of up to 10% for 2048-bit RSA on some platforms.

## 7 Related Work

Agat proposes a program transformation for removing control-flow timing leaks by equalizing branches of conditionals with secret guards [1], with follow-up work in [5, 18]. In an accompanying technical report [2] Agat presents the implementation of the transformation in Java bytecode, which includes an informal discussion of the effect of instruction and data caches on the security of the transformation. Our approach relies on lower-level models, namely x86 executables and simple but accurate cache models, based on which we can prove the security of cache-aware programming.

Molnar et al. [20] propose a program transformation that eliminates branches on secret to remove leaks due to control flow and instruction caches, together with a static check for the resulting x86 executables. Our approach is more permissive than theirs that it can establish the security of code that contains restricted forms of secret-dependent control flow and memory access patterns. It is worth emphasizing that the increased permissiveness of our approach comes from the fact that we rely on models of the hardware architecture for our analysis. If no such models are available, the safe way to go is to forbid all kinds of secret-dependent behavior.

Doychev et al. [10] develop the CacheAudit static analyzer for cache side-channels, which we utilize for our analyses. The capabilities of CacheAudit however do not allow reasoning about dynamic memory addresses, which limits the scope of the analysis mostly to symmetric cryptography, and their analysis is limited to weaker models of adversaries who can observe the final cache states or traces of cache hits and misses.

Coppens et al. [8] investigate mitigations for timing-based side channels on x86 architecture, and they identify new side channels in programs without secret-dependent memory lookups due to out-of-order execution. In contrast, we prove the security of countermeasures. For this we rely on accurate models of caches, but we do not take into account out-of-order execution.

Bernstein et al. advocate defensive programming [6] that avoids all secret-dependent memory lookups and branching and demonstrate the practicality of their pro-

posal with NaCl. Almeida et al. develop a static analyzer that can automatically confirm that programs follow that regime [3]. Barthe et al. [4] establish that adhering to that policy provides security against very strong adversary models.

Langley [15] shows how to perform a dynamic analysis based on Valgrind and memcheck. His technique flags the secret-dependent (but cache-line independent) memory lookups of the OpenSSL sliding window-based modular exponentiation as a potential leak. Our technique gives more fine-grained insights about its security, including proofs of security for adversaries that can observe memory accesses only at the granularity of memory blocks.

## 8 Conclusions

In this paper we devise novel techniques that provide support for bit-level and arithmetic reasoning about pointers in the presence of dynamic memory allocation. These techniques enable us to perform the first rigorous analysis of widely deployed software countermeasures against cache attacks on modular exponentiation, based on executable code.

## References

- [1] J. Agat. Transforming out timing leaks. In *POPL 2000*, pages 40–53. ACM, 2000.
- [2] J. Agat. Transforming out timing leaks in practice: An experiment in implementing programming language-based methods for confidentiality, 2000.
- [3] J. B. Almeida, M. Barbosa, J. S. Pinto, and B. Vieira. Formal verification of side-channel countermeasures using self-composition. *Sci. Comput. Program.*, 78(7):796–812, 2013.
- [4] G. Barthe, G. Betarte, J. Campo, C. Luna, and D. Pichardie. System-level non-interference for constant-time cryptography. In *Proceedings of the 2014 ACM SIGSAC Conference on Computer and Communications Security*, pages 1267–1279. ACM, 2014.
- [5] G. Barthe, T. Rezk, and M. Warnier. Preventing Timing Leaks Through Transactional Branching Instructions. In *Proc. 3rd Workshop on Quantitative Aspects of Programming Languages (QAPL 2006)*, Electronic Notes in Theoretical Computer Science (ENTCS), pages 33–55. Elsevier, 2005.
- [6] D. J. Bernstein, T. Lange, and P. Schwabe. The security impact of a new cryptographic library. In *LATINCRYPT*, pages 159–176. Springer, 2012.
- [7] D. Cock, Q. Ge, T. Murray, and G. Heiser. The last mile: An empirical study of timing channels on sel4. In *CCS*. ACM, 2014.
- [8] B. Coppens, I. Verbauwhede, K. D. Bosschere, and B. D. Sutter. Practical mitigations for timing-based side-channel attacks on modern x86 processors. In *SSP*, pages 45–60. IEEE, 2009.
- [9] P. Cousot and R. Cousot. Abstract interpretation: a unified lattice model for static analysis of programs by construction of approximation of fixpoints. In *POPL*, pages 238–252, 1977.
- [10] G. Doychev, B. Köpf, L. Mauborgne, and J. Reineke. Cacheaudit: A tool for the static analysis of cache side channels. *ACM Transactions on Information and System Security*, 18(1):4:1–4:32, June 2015.
- [11] S. Dziembowski and K. Pietrzak. Leakage-resilient cryptography. In *FOCS*. IEEE, 2008.
- [12] S. Gueron. Efficient software implementations of modular exponentiation. *J. Cryptographic Engineering*, 2(1):31–43, 2012.
- [13] T. Kim, M. Peinado, and G. Mainar-Ruiz. StealthMem: System-level protection against cache-based side channel attacks in the cloud. In *19th USENIX Security Symposium*. USENIX, 2012.
- [14] B. Köpf and A. Rybalchenko. Approximation and randomization for quantitative information-flow analysis. In *CSF*, pages 3–14. IEEE, 2010.
- [15] A. Langley. Checking that functions are constant time with valgrind. <https://www.imperialviolet.org/2010/04/01/ctgrind.html>, 2010. Accessed: 6 March 2016.
- [16] F. Liu, Y. Yarom, Q. Ge, G. Heiser, and R. B. Lee. Last-level cache side-channel attacks are practical. In *IEEE Symposium on Security and Privacy*, pages 605–622. IEEE Computer Society, 2015.
- [17] G. Lowe. Quantifying Information Flow. In *Proc. 15th IEEE Computer Security Foundations Symposium (CSFW 2002)*, pages 18–31. IEEE, 2002.
- [18] H. Mantel and A. Starostin. Transforming out timing leaks, more or less. In *ESORICS*, pages 447–467. Springer, 2015.
- [19] J. L. Massey. Guessing and Entropy. In *Proc. 1994 IEEE Symposium on Information Theory (ISIT 1994)*, page 204. IEEE, 1994.
- [20] D. Molnar, M. Piotrowski, D. Schultz, and D. Wagner. The program counter security model: Automatic detection and removal of control-flow side channel attacks. In *Information Security and Cryptology-ICISC 2005*, pages 156–168. Springer, 2006.
- [21] G. Smith. On the foundations of quantitative information flow. In *FoSSaCS*. Springer, 2009.
- [22] Z. Wang and R. B. Lee. A novel cache architecture with enhanced performance and security. In *41st IEEE/ACM Intl. Symposium on Microarchitecture (MICRO)*, pages 83–93, 2008.
- [23] Y. Yarom and K. Falkner. FLUSH+RELOAD: A high resolution, low noise, L3 cache side-channel attack. In *USENIX Security Symposium*. USENIX Association, 2014.
- [24] Y. Yarom, D. Genkin, and N. Heninger. Cachebleed: A timing attack on openssl constant time rsa. *Cryptology ePrint Archive, Report 2016/224*, March 2016. <http://eprint.iacr.org/>.
- [25] Y. Zhang, A. Juels, M. K. Reiter, and T. Ristenpart. Cross-VM side channels and their use to extract private keys. In *CCS*. ACM, 2012.